# Molecular Dynamics of Complexes of Atosiban with Neurohypophyseal Receptors in the Fully Hydrated Phospholipid Bilayer

**Magdalena J. Ślusarz[a]*, Rafał Ślusarz[a], Robert Meadows[b], Jerzy Trojnar[b] and Jerzy Ciarkowski[a]**

[a] Faculty of Chemistry, University of Gdańsk, Sobieskiego 18, 80-952 Gdańsk, Poland
[b] Ferring Research Institute Inc, 3550 General Atomics Court, Bldg. 2, San Diego, CA 92121, USA

**Full Paper**

The aim of our research was to get insight into the molecular mechanism of binding atosiban, a strong selective oxytocin (OT) antagonist by OT receptor (OTR) versus vasopressin V1a and V2 receptors (V1aR and V2R, respectively). The docking of ligand and interaction with receptor are dynamic events and Molecular Dynamics (MD) seems to be a proper tool for studying the mentioned processes. Therefore we describe MD of three pairs of atosiban-receptor complexes, two complexes per each receptor, conducted in the fully hydrated 1-palmitoyl-2-oleoyl-*sn*-glycero-3-phosphatidylcholine lipid bilayer, simulating G protein-coupled receptors environment. We confirmed strong and specific binding of atosiban in OTR and a weaker binding of it in V1aR, on the contrary to its less specific binding in V2R, in the agreement with our preliminary results [Ślusarz et al. 2003].

## 1 Introduction

The neurohypophyseal hormone oxytocin (CYIQNCPLG-$NH_2$, OT) is synthesized in hypothalamus, from where it is transported to the posterior lobe of the pituitary gland for secretion into the blood. OT is composed of a heterodetic cyclohexapeptide (due to the disulfide $Cys^1$ – $Cys^6$ bridge; the tocin ring) and the three-residue C-terminal tail. OT is crucial for the stimulation of uterus contractions during labor and secretion of milk during lactation [1, 2]. The both biological effects result from stimulation of OT receptors (OTR) in mammalian uterine smooth muscles and myoepithelial cells in mammary gland [3, 4, 5], respectively. The sequence of OTR was reported in 1992 [6]. Oxytocin receptors are members of the class A G protein-coupled receptor (GPCR) family. The latter are integral membrane proteins consisting of seven hydrophobic transmembrane α-helices (TM) successively connected with alternating extracellular (EL) and intracellular (IL) hydrophilic loops, beginning with an extracellular N-terminus and ending with a cytoplasmatic C-terminus [7, 8]. In the whole class A family helices TM2-TM7 are involved in ligand binding and they are so arranged as to form a ligand binding pocket [9, 10, 11]. GPCRs are targets for biogenic substances like hormones, neurotransmitters, neuromodulators, odorants and they are also targets for over 50% of all drugs [12, 13, 14, 15]. Development of new, more selective OTR antagonists thus is important for design of drugs preventing preterm labor and regulating dysmenorrhea [16].

In our previous study we determined binding domains of the OT, V1a and V2 receptors interacting with the OT antagonist atosiban, [$Mpa^1$,D-$Tyr(Et)^2$,$Thr^4$,$Orn^8$]OT (Mpa: 3-mercaptopropionic acid; Orn: ornithine), (Figure 1) [17]. Atosiban is a competitive antagonist of uterine OTreceptors [18, 19] used in the treatment of preterm labor [20, 21, 22, 23, 24, 25, 26, 27]. In this paper we describe six (1 ns each) molecular dynamic (MD) simulations of atosiban – neurohypophyseal receptor complexes, embedded in the fully hydrated phospholipid bilayer. Today, simulations in mem-

* To receive all correspondence

**Key words:** atosiban, GPCR, molecular dynamics, phospholipid bilayer

**Abbreviations:** CSA – Constrained Simulated Annealing; EL – extracellular loop; GPCR – G protein-coupled receptor; IL – intracellular loop; MD – molecular dynamics; Mpa – 3-mercaptopropionic acid; Orn - ornithine; OT – oxytocin; OTR – oxytocin receptor; PAL – palmitoyl; PME – Particle Mesh Ewald; POPC – 1-palmitoyl-2-oleoyl-*sn*-glycero-3-phosphatidylcholine; SCI – Scalable Coherent Interface; TM – transmembrane α-helice; V1aR – vasopressin V1a receptor; V2 – vasopressin V2 receptor; 7TM – heptahelical transmembrane domain

 DOI: 10.1002/qsar.200430888 © 2004 WILEY-VCH Verlag GmbH & Co. KGaA, Weinheim

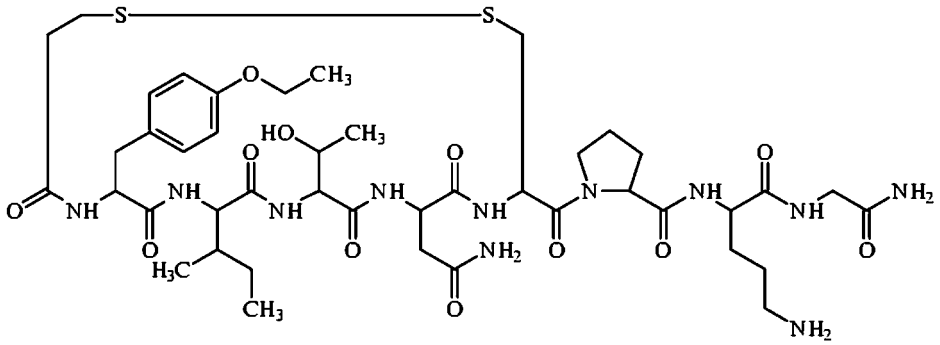

**Figure 1.** Atosiban ([Mpa[1],D-Tyr(Et)[2],Thr[4],Orn[8]]OT); Mpa – 3-mercaptopropionyl, Orn – ornithine, OT – oxytocin;

brane are commonplace, with recent reports of trajectory lengths even of 10 ns [28]. They include Particle Mesh Ewald (PME) summation method [29, 30, 31] for the accurate calculation of Coulombic intermolecular forces between phospholipid headgroups and water, as well as constant pressure, that allows dynamic adaptation of membrane size and shape.

The docking of ligand and receptor activation (or inhibition) are dynamic events, which are poorly described by a static model, that we presented in our previous paper [17]. Therefore here we describe 1ns MD, being a much better tool for studying the mentioned processes. MD simulation of receptor-atosiban complexes explores geometry, location and orientation of ligand docked into the receptors. Besides, 1ns MD simulation makes possible significant movements of the receptor protein such as helices and loops motions induced by docking ligand.

The aim of our research was to get insight into the molecular mechanism of binding atosiban by OTR versus vasopressin V1a and V2 receptors (V1aR and V2R, respectively). The MD simulation in the fully hydrated phospholipid bilayer served us for investigation these interactions and verification our preliminary results [17].

## 2 Methods

Receptor model building, ligand docking and constrained simulated annealing (CSA) for preliminary relaxation of the systems were done as described [17]. So was the selection, after CSA, of the six complexes with the lowest energy (a pair per each receptor) [17]. Subsequently, they were inserted into the phospholipid bilayer. 1-palmitoyl-2-oleoyl-*sn*-glycero-3-phosphatidylcholine (POPC) membrane model consisting of 120 POPC lipid molecules in two layers, of over 7000 water molecules (slightly varying in number, depending on the shape of individual receptors), and of $Cl^-$ counterions (to neutralize the charge of the complexes) was used. The hydrated POPC phospholipid bilayer mimics a GPCR environment with three diverse regions: a hydrophobic interior formed by the fatty acid hydrocarbon tails, polar regions on both sides formed by the phosphatidylcholine head groups, and water regions. Due to the use of the bilayer the transmembrane helices and loops could freely move in the membrane.

Insertion of six selected complexes into bilayer was accomplished using previously modeled and fully equilibrated phospholipid-receptor models [32, 33] wherefrom the original receptors had been replaced with the current ones. This was possible because the shapes of the former and current receptor were almost identical.

The periodic box ready to be modeled had 75.7 Å × 64.1 Å × 84.9 Å initial size for OTR complexes, 75.9 Å × 64.0 Å × 84.5 Å for V1aR complexes and 75.1 Å × 63.3 Å × 85.4 Å for V2R complexes, see Figure 2.

Molecular dynamics followed by energy minimization was carried out using the AMBER 5.0 package [34]. For POPC, receptors and ligand, the OPLS [35] united atom

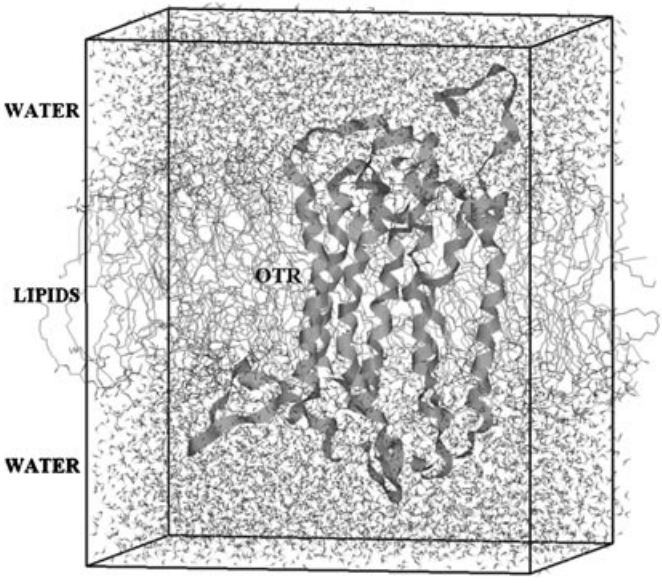


**Figure 2.** Representation of the periodic box used in MD simulations. OT receptor embedded in the phospholipid (POPC) bilayer has been shown.

 © 2004 WILEY-VCH Verlag GmbH & Co. KGaA, Weinheim 

parameters were applied. All systems were simulated for 1ns using PME summation [29, 30, 31]. To prevent unfolding or any other unwanted modifications of the TM helices, flat-bottom soft harmonic-wall restraints were imposed onto the φ, ψ and ω peptide angles of the TM amino acid residues. These restraints, held for the whole simulation and centered around the initial φ, ψ and ω torsion, were defined in AMBER as 800 kcal · (mol · deg)$^{-1}$, with the angle limits: −20, −10, +10, +20 degrees for the φ and ψ angles, and −15, −5, +5, +15 degrees for the ω angles values, and resulted in about 100 kcal · (mol · deg)$^{-1}$ effective penalty per each of these torsions. The amino acid residues contributing to transmembrane α helices as well as palmitoylation sites and disulfide bridges in the OT, V1a and V2 receptors are given in Table 1. The dynamics were carried out in accordance with the following protocol: step 1 – 20 ps – linear heating from 0 to 300 K, with positional TM $C^{\alpha}$ constraints. Step 20 – 100 ps – positional TM $C^{\alpha}$ constraints (belly) at constant 300 K. Step 100 – 160 ps – positional TM $C^{\alpha}$ constraints gradually and simultaneously in each of 7 TM helices released: every two $C^{\alpha}$ atoms from N- and C-terminal pairs per every 10 ps, until complete release at 160 ps of simulation. Step 160 – 1000 ps – position-unconstrained dynamics at constant 300 K. There were also geometry restraints imposed on *cis*-bonds in lipids forming the membrane. They were defined in AMBER at the level of 400 kcal · (mol · deg)$^{-1}$ and resulted in effective torsion penalty of about 100 kcal · (mol · deg)$^{-1}$ as previously. The positional TM $C^{\alpha}$ constraints used at the same beginning of the simulation were necessary to retain the proper three-dimensional structure of the receptor protein. After molecular docking and geometry optimization we obtained stable, relaxed structure at the temperature near 0 K. Energy that is provided during linear heating to the temperature 300 K at the beginning of MD is sufficient for degeneration of helical structure of receptor protein. The positional constraints on TM $C^{\alpha}$ had prevented the helices from degeneration and then imposed constraints was being gradually removed. This is standard AMBER procedure [34].

The last step consisted of the relaxation of the complexes using a constrained simulated annealing protocol (CSA) *in vacuo* for 15 ps, followed by energy minimization [36, 37], with positional constrains on $C^{\alpha}$ atoms in transmembrane domains to enable the system(s) final intra- and intermolecular relaxations and geometry optimization. The CSA protocol consisted of heating the system up to 1200 K for 1 ps, leaving this temperature for another 2 ps, and re-cooling the system to low temperatures during final 12 ps.

All the calculations were carried out on a 128-processor SMP cluster of Pentium III Xeon 700 MHz computers linked in the SCI (Scalable Coherent Interface) fast network.

## 3 Results

We obtained three pairs of relaxed receptor-atosiban complexes, a pair per each receptor. In all complexes, a location of atosiban, compatible with polarity of a binding pocket, has been retained. The C-terminal part of atosiban, strongly hydrophilic due to Orn8, was turned towards hydrophilic entrance of the binding pocket. In contrast, the hydrophobic N-terminus of the peptide approached the hydrophobic floor of the pocket [17]. In Figure 3 the binding pockets of OTR, V1aR and V2R are given. Only a more horizontal location of atosiban in V2R breaks this rule, which may be a result of a small difference in the size of the pocket – this being somewhat wider and shallower in V2R than in V1aR and OTR. Such atosiban locations may suggest less specific binding of atosiban by V2R, contrary to its stronger and more specific binding by OTR and less strong by V1aR, see below.

One complex per each receptor, that of lower energy in any pair, were eventually selected for further detailed examination. Receptor amino acid residues involved in atosiban binding were identified using the distance criteria. Thus, all amino acid residues of respective residues whose nearest atom was not farther then 2.5 Å from whatever atoms in the atosiban amino acid residues were considered interacting with the ligand. Amino acid residues meeting these criteria are listed in Table 2 and presented in Figure 3, where atosiban location inside the binding domain and the

**Table 1.** The numbers of amino acid residues forming the a-helical transmembrane domains (TM), disulfide bridge (S – S) as well as palmitoylation sites (PAL) in OT, V1a and V2 receptors.

| | OT | V1aR | V2R |
|---|---|---|---|
| **TM1** | 37 – 66 | 49 – 78 | 35 – 64 |
| **TM2** | 73 – 102 | 85 – 114 | 73 – 102 |
| **TM3** | 109 – 141 | 121 – 153 | 109 – 141 |
| **TM4** | 151 – 173 | 165 – 187 | 154 – 176 |
| **TM5** | 197 – 222 | 213 – 238 | 202 – 227 |
| **TM6** | 270 – 300 | 286 – 316 | 266 – 296 |
| **TM7** | 309 – 329 | 328 – 348 | 305 – 325 |
| **PAL** | 346 | 365 | 341 |
| | 347 | 366 | 342 |
| **S – S** | 112 – 187 | 124 – 203 | 112 – 282 |


© 2004 WILEY-VCH Verlag GmbH & Co. KGaA, Weinheim

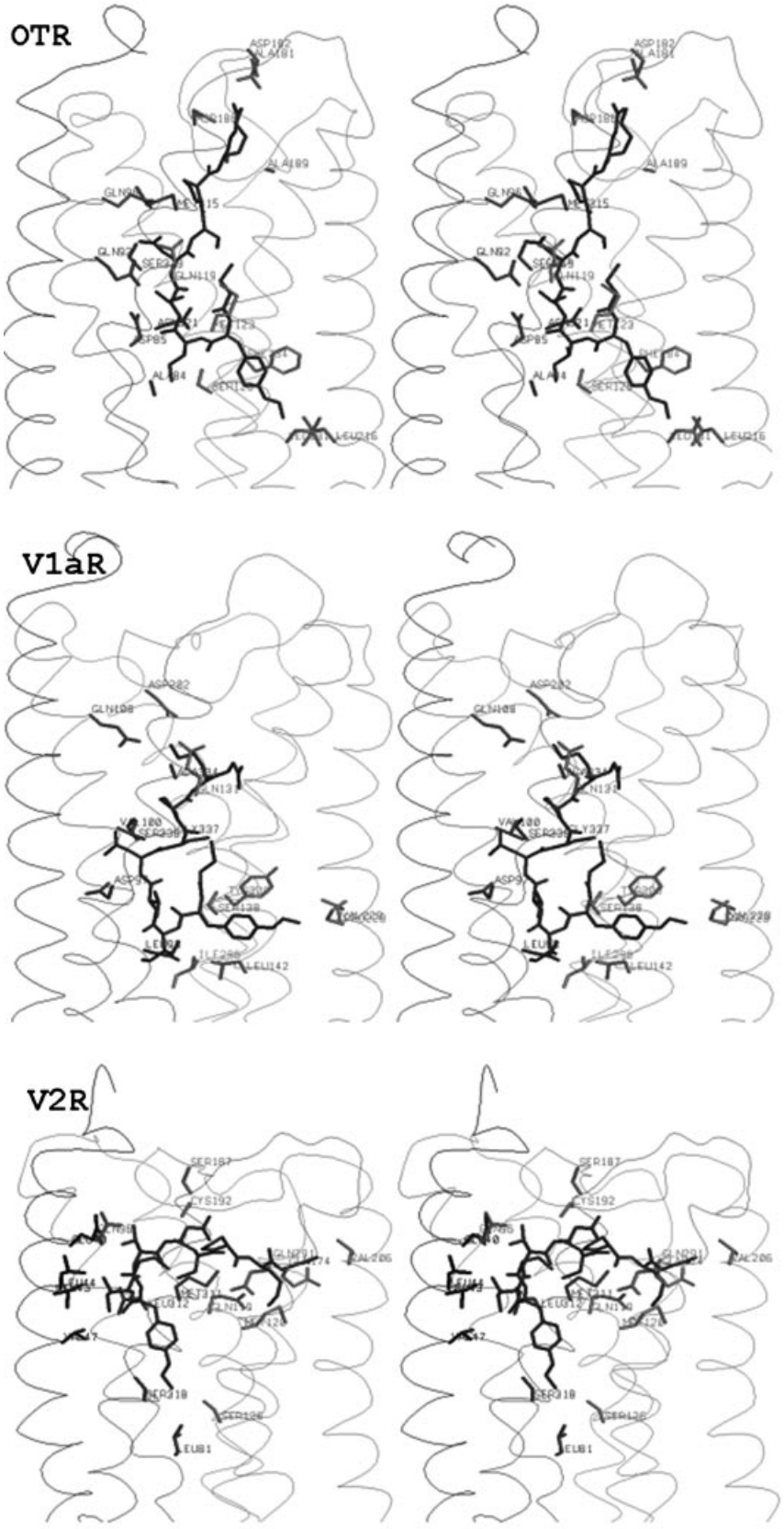


**Figure 3.** Stereodiagrams of the final atosiban-neurohypophyseal receptors complexes. Only the receptor extracellular halves are shown. The binding amino acid residues are marked and their side chains exposed.

 © 2004 WILEY-VCH Verlag GmbH & Co. KGaA, Weinheim 

**Table 2.** Amino acid residues most involved in atosiban binding. Those in common rows (exc. El2) occupy equivalent positions in the TM helices.

| | OTR | V1aR | V2R |
|---|---|---|---|
| **TM1** | | | Glu40 |
| | | | Leu43 |
| | | | Leu44 |
| | | | Val47 |
| | – | Leu93 | Leu81 |
| **TM2** | Ala84 | – | – |
| | Asp85 | Asp97 | – |
| | – | Val100 | – |
| | Gln92 | – | – |
| | Gln96 | Gln108 | Gln95 |
| **TM3** | Gln119 | Gly131 | Gln119 |
| | – | – | Met120 |
| | Met123 | – | – |
| | Set126 | Ser138 | Ser126 |
| | Leu131 | Leu142 | – |
| **TM4** | | | Gln174 |
| **TM5** | – | – | Val206 |
| | – | Pro228 | – |
| | – | Val229 | – |
| | Leu216 | – | – |
| **TM6** | – | – | Gln291 |
| | – | Ile296 | – |
| | Phe284 | Tyr300 | – |
| **TM7** | Met315 | Ala334 | Met311 |
| | – | – | Leu312 |
| | – | Gly337 | – |
| | Ser319 | Ser338 | – |
| | Asn321 | – | – |
| | – | – | Ser318 |
| **EL2** | Ala181 | | Ser187 |
| | Asp182 | Asp202 | Cys192 |
| | Asp186 | | |
| | Ala189 | | |

interacting amino acid residues of the receptor are shown. One can see a salt bridge between atosiban Orn8 and Asp from the second extracellular loop (EL2) in OTR and V1aR. In OTR the EL2 Asp182 is about 1.75 Å away from the to atosiban Orn8 while in V1aR the equivalent distance (involving receptor Asp202) equals to 1.65 Å, this interaction is absent in V2R. Another interaction resembling a stacking effect between the phenyl ring of D-Tyr(Et)2 in the ligand and the aromatic TM6 residues of the receptor (in OTR with Phe284 and in V1aR with Tyr300), see Table 2, is observed. There are also dispersion interactions between atosiban Ile3 residue and receptor hydrophobic residues: Ala84 from TM2, Ser126 from TM3 in OTR; Leu93 and Leu142 from TM3, Ile296 from TM6 in V1aR; and Leu43, Leu44, Val47 from TM1 and Leu312 from TM7 in V2R; interactions between the ethoxy- part of atosiban D-Tyr(Et)2 and Leu131 from TM3, Leu216 from TM5 in OTR; Pro228, Val229 from TM5 in V1aR; and Leu81 from TM2 and Ser126 from TM3 in V2R. The atosiban disulfide bond interacts with hydrophobic receptor amino acid residues: Met123 from TM3 in OTR; and Gly337 from TM7 in V1aR. In these complexes there is a possibility of formation of hydrogen bonds, among others: in the OT receptor involving the Thr4 OH with a side chain oxygen of Asp85 from TM2 at the distance of 1.8 Å, the backbone oxygen of Orn8 with an amide hydrogen of Ala189 from EL2 at the distance of 2.4 Å, the side chain amide hydrogen of Asn5 with a side chain oxygen of Ser319 from TM7 at the distance of 2.0 Å; and the backbone oxygen Thr4 with a side chain amide hydrogen of Asn321 from TM7 at the distance of 2.0 Å. In the V1a receptor involving accordingly: the side chain hydrogen of Asn5 with the side chain oxygen of Asp97 from TM3 at the distance of 1.8 Å, the oxygen of Mpa1 with the side chain hydrogen of Ser138 from TM3 at the distance of 1.8 Å, the side chain oxygen of Asn5 with the side chain hydrogen of Ser338 from TM7 at the distance of 1.7 Å. And finally in the V2 receptor involving only the side chain hydrogen of Asn5 with a side chain oxygen of Ser187 from EL2 at the distance of 1.9 Å. The all interactions listed above and those less significant ones are shown on the maps (Figures 4, 5, 6, for OTR, V1aR and V2R respectively).


© 2004 WILEY-VCH Verlag GmbH & Co. KGaA, Weinheim

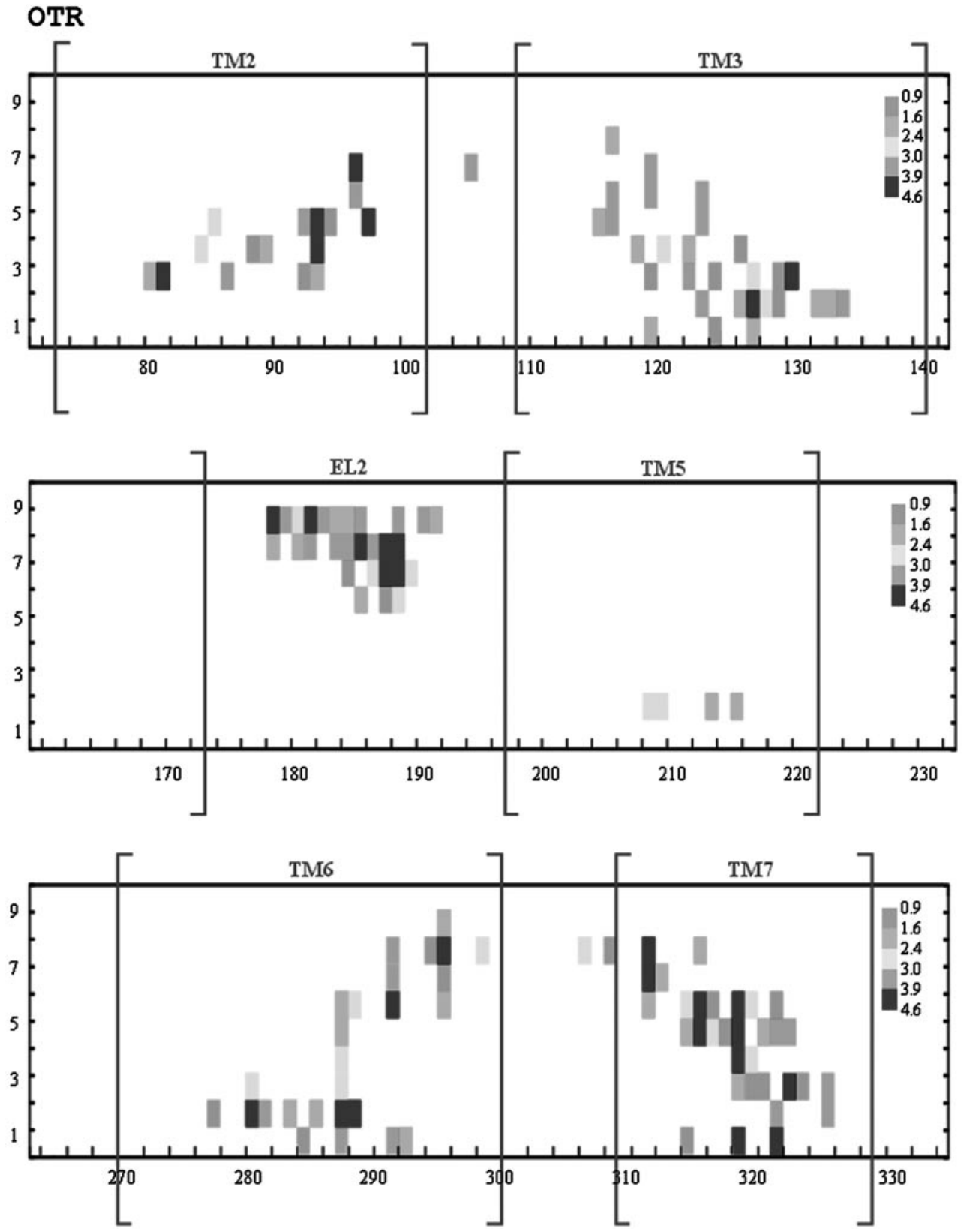


**Figure 4.** The maps of OTR-atosiban contacts. The contours represent the closest distances between pairs of residues in accordance with the scale on the right (distances are in Angstroms). Horizontal axes: residues of receptor. Vertical axes: ligand amino-acid residues.

 © 2004 WILEY-VCH Verlag GmbH & Co. KGaA, Weinheim 

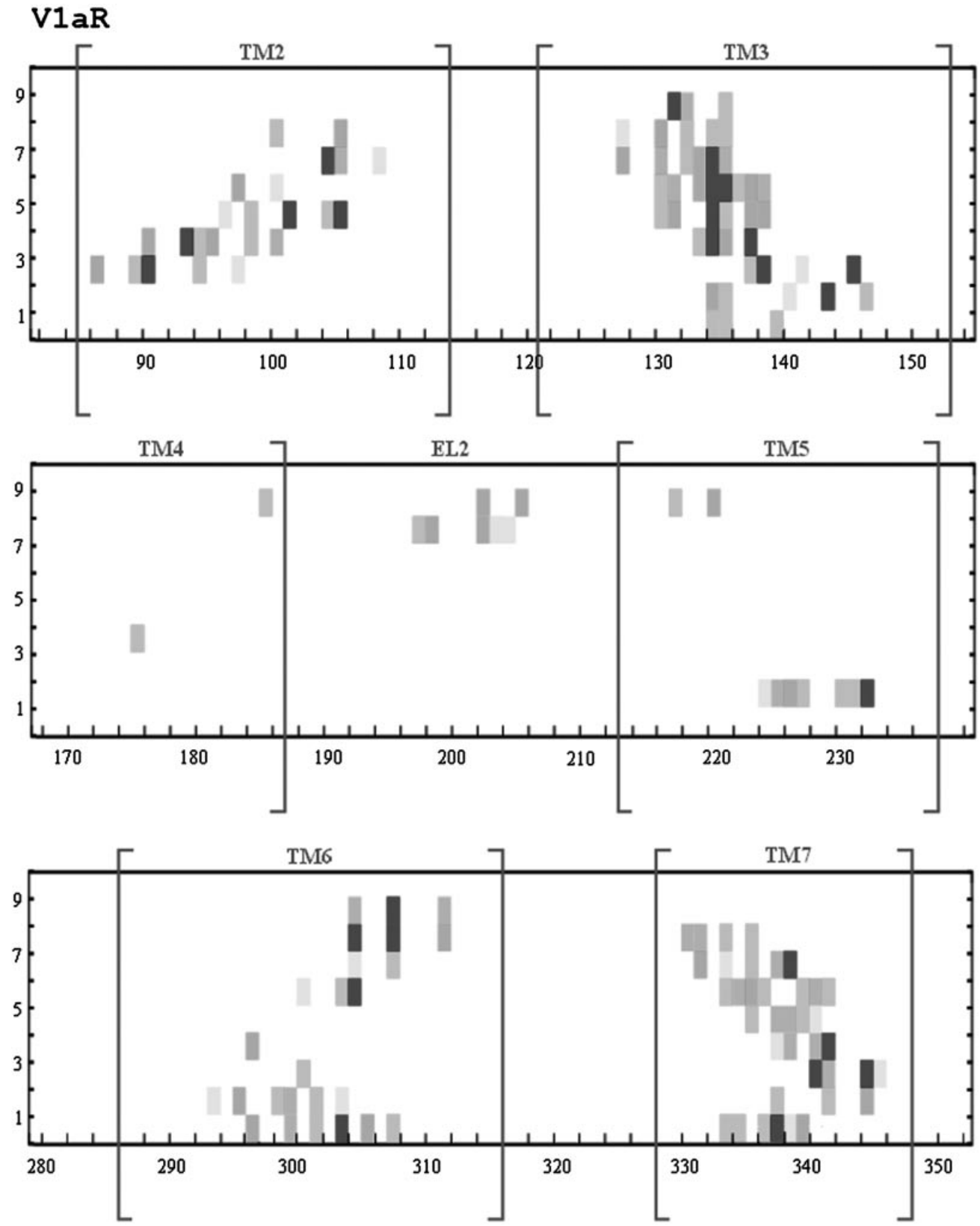


**Figure 5.** The maps of V1aR-atosiban contacts. The contours represent the closest distances between pairs of residues in accordance with the scale on the right (distances are in Angstroms). Horizontal axes: residues of receptor. Vertical axes: ligand amino-acid residues.


© 2004 WILEY-VCH Verlag GmbH & Co. KGaA, Weinheim

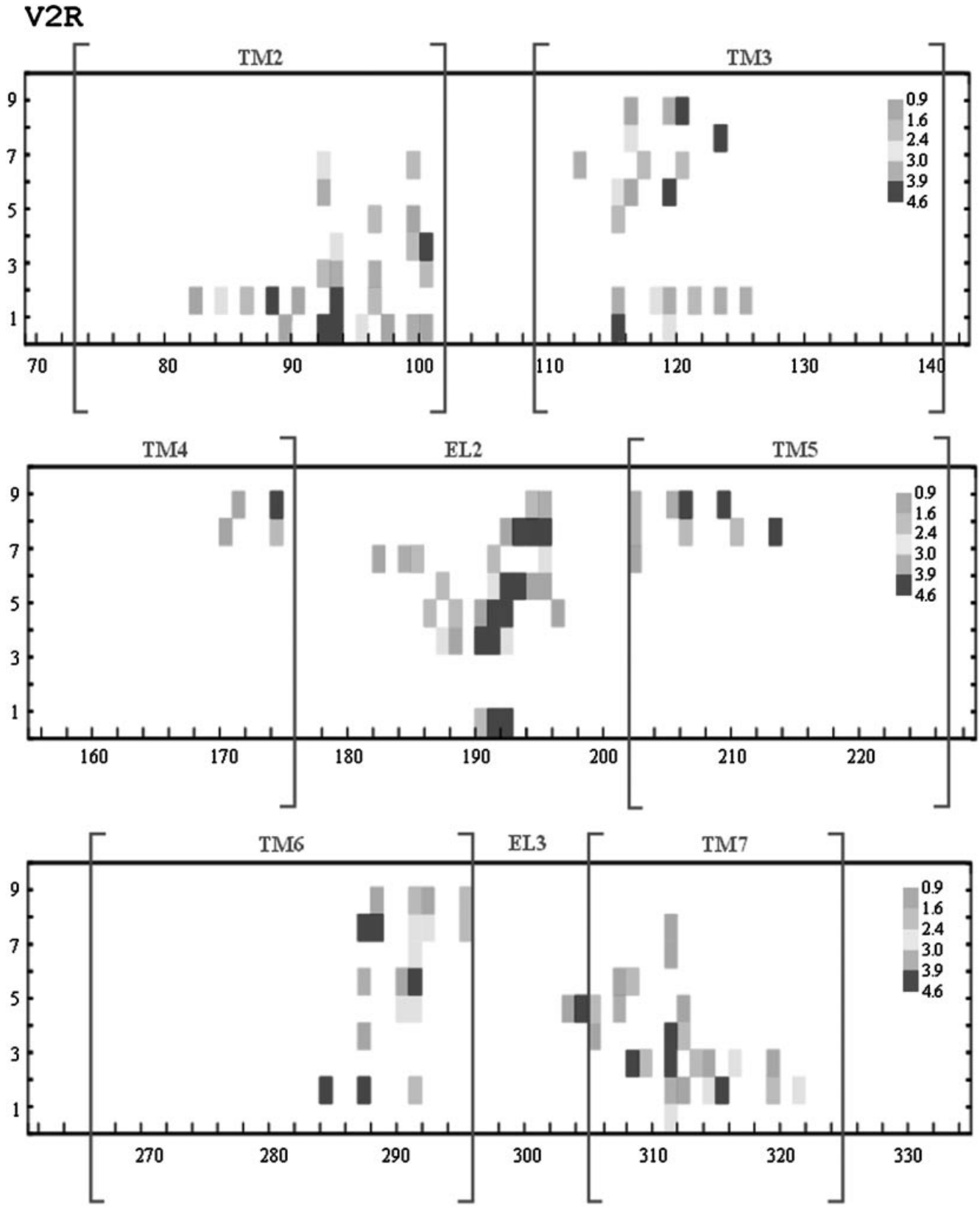


**Figure 6.** The maps of V2R-atosiban contacts. The contours represent the closest distances between pairs of residues in accordance with the scale on the right (distances are in Angstroms). Horizontal axes: residues of receptor. Vertical axes: ligand amino-acid residues.


© 2004 WILEY-VCH Verlag GmbH & Co. KGaA, Weinheim

## 4 Discussion

Given both this and the preliminary work [17], one can see that atosiban binds at the same site in the central cleft of all receptors, but the orientation of molecule is different in the OT and V1a versus the V2 receptors. As mentioned previously – the different positions of ligand in the binding pocket of V2R can result from a difference in the structure and size of binding cavity in V2R versus V1aR and OTR. Observed interactions between atosiban and V2R do not seem to be specific, as we have already pointed out, thus, below we discuss only interaction with the OT and V1a receptors.

Orientation of atosiban in the binding pockets of OTR and V1aR is compatible with polarity of atosiban and binding sites of the receptors. In the Class A GPCRs non-polar amino acid residues form the bottom of binding cavity, whereas loops (especially EL2), containing polar amino acid residues, make the entrance of this binding place. Compared with oxytocin, atosiban molecule is more hydrophobic at the N-terminus (Cys1 in oxytocin is replaced with Mpa1) so the tocin ring and especially the first three amino acid part of atosiban (Mpa1, D(Tyr)Et2, Ile3) are placed at the bottom of the binding pocket and interact with hydrophobic amino acid residues from the TM helices, see Figure 3 – 6 and Table 2. On the other hand the C-terminal tail of atosiban is strongly polar due to the replacement of Leu8 (present in OT) with Orn8. Most important, Asp(EL2), forming a salt bridge with Orn8, was identified.

This dual polarity of atosiban, strongly enhanced relative to OT, presumably allows the antagonist to fit tighter into the receptor binding site then OT. This feature of atosiban interaction with OTR may provide an important point to understanding the mechanism of its binding and selectivity. We suppose, that aspartic acid in EL2 may provide a handle (anchor) catching Orn8 of the ligand, approaching from the extracellular side. Once the ionic bridge is formed, the ligand enters the binding pocket of the receptor and then EL2 covers the binding cavity. This binding is supported by a strong attraction of the N-terminal hydrophobic part of atosiban by hydrophobic receptor amino acid residues in the lower part of binding pocket. This hypothesis can be confirmed by molecular dynamics simulations of similar ligand-receptor interactions [38].

Formation of the salt bridge is in our opinion the most essential interaction which may be critical in binding of atosiban and similar ligands to neurohypophyseal receptors. The non-polar interactions in the binding pocket may also be crucial for atosiban-receptor selectivity, especially stacking between the phenyl rings and contacts of the N-terminal atosiban residues like Ile3 or D-Tyr(Et)2, incl. its ethoxy part. These interactions occur in OTR and V1aR only, thus we confirmed strong and specific binding of atosiban with OTR and weaker binding of it in V1aR, on the contrary to its less specific binding in V2R, in agreement with our preliminary results [17] and experimental data [20, 21, 22, 23, 24, 25, 26, 27].

These findings could potentially help in the design of new potent and selective OTR antagonists.

## References

[1] C. Barberis, B. Mouillac, T. Durroux, *J. Endocrinol.* **1998**, *156*, 223 – 229.
[2] C. Barberis, E. Tribollet, *Crit. Rev. Neurobiol.* **1996**, *10,* 119 – 154.
[3] G. Gimpl, F. Fahrenholtz, *Physiol. Rev.* **2001**, *81,* 629 – 683.
[4] J. Peter, H. Burbach, R. A. Adan, S. J. Lolait, F. W. Van Leeuwen, E. Mezey, M. Palkovits, C. Barberis, *Cell. Mol. Neurobiol.* **1995**, *15*, 573 – 595.
[5] H. H. Zingg, *Baillieres Clin. Endocrinol. Metab.* **1996**, *10*, 75 – 96.
[6] T. Kimura, O. Tanizawa, K. Mori, M. J. Brownstein, H. Okayama, *Nature* **1992**, *356*, 526 – 529.
[7] R. E. Stenkamp, D. C. Teller, K. Palczewski, *Chembiochem*. **2002**, *3*, 963 – 967.
[8] J. A. Ballesteros, L. Shi, J. A. Javitch, *Mol. Pharmacol*. **2001**, *60*, 1 – 19.
[9] D. C. Teller, T. Okada, C. A. Behnke, K. Palczewski, R. E. Stenkamp, *Biochemistry* **2001**, *40*, 7761 – 7772.
[10] T. P. Sakmar, *Curr. Opin. Cell Biol.* **2002**, *14*, 189 – 195.
[11] B. W. Koenig, *Chembiochem*. **2002**, *3*, 975 – 980.
[12] Y. Hakak, D. Shrestha, M. C. Goegel, D. P. Behan, D. T. Chalmers, *FEBS Lett.* **2003**, *550*, 11 – 17.
[13] O. M. Becker, S. Shacham, Y. Marantz, S. Noiman, *Curr. Opin. Drug Discov. Devel.* **2003**, *6*, 353 – 361
[14] S. J. Dowell, A. J. Brown, *Receptors Channels* **2002**, *8*, 343 – 352.
[15] J. Ballesteros, K. Palczewski, *Curr. Opin. Drug Discov. Devel.* **2001**, *4*, 561 – 574.
[16] P. D. Williams, M. G. Bock, B. E. Evans, R. M. Freidinger, D. J. Pettibone, *Adv. Exp. Med. Biol.* **1998**, *449*, 473 – 479.
[17] M. J. Ślusarz, R. Ślusarz, R. Kaźmierkiewicz, J. Trojnar, K. Wiśniewski, J. Ciarkowski, *Protein Pept. Lett.* **2003**, *10*, 295 – 302.
[18] M. Akerlund, P. Stromberg, A. Hauksson, L. F. Andersen, *Br. J. Obstet. Gynaecol.* **1987**, *94*, 1040 – 1044.
[19] P. Melin, J. Trojnar, B. Johansson, H. Vilhard, M. Akerlund, *J. Endocrinol.* **1986**, *11*, 125-131.
[20] A. Herbst, D. Wide-Swensson, I. Ingemarsson, *Eur. J. Obstet. Gynecol. Reprod. Biol.* **2003**, *108*, 109 – 110.
[21] I. Ingemarsson, R. F. Lamont, *Acta Obstet. Gynecol. Scand.* **2003**, *82*, 1 – 9.
[22] H. Helmer, M. Brunbauer, K. Rohrmeister, *BJOG* **2003**, *110* Suppl *20*, 113 – 115.
[23] E. Menthonnex, P. Menthonnex, *J. Gynecol. Obstet. Biol. Reprod. (Paris)* **2003**, *32*, 157 – 168.
[24] H. Nissel, K. Wolff, *BJOG* **2003**, *110*, 89.
[25] M. Akerlund, *Prog. Brain. Res.* **2002**, *139*, 359 – 365.
[26] A. Coomarasamy, E. M. Knox, H. Gee, K. S. Khan, *Med. Sci. Monit.* **2002**, *8*, 268 – 273.
[27] P. Husslein, *Acta. Obstet. Gynecol. Scand.* **2002**, *81*, 633 – 641.
[28] U. Essmann, M. L. Berkowitz, *Biophys. J.* **1999**, *76*, 2081 – 2089.
[29] P. P. Ewald, *Ann. Phys.* **1921**, *64*, 253 – 287.
[30] T. Darden, D. York, L. Petersen, *J. Chem. Phys.* **1993**, *98*, 10089 – 10092.
[31] U. Essmann, L. Perera, M. L. Berkowitz, T. Darden, H. Lee, L. G. Pedersen, *J. Chem. Phys.* **1995**, *103*, 8577 – 8593.


© 2004 WILEY-VCH Verlag GmbH & Co. KGaA, Weinheim

[32] K. Murzyn, T. Róg, G. Jezierski, Y. Takaoka, M. Pasenkiewicz-Gierula, *Biophys. J.* **2001**, *81*, 170 – 183.
[33] M. Pasenkiewicz-Gierula, K. Murzyn, T. Róg, C. Czaplewski, *Acta Biochim. Polon.* **2000**, *47*, 601 – 611.
[34] D.A Pearlman, D. A. Case, J. W. Caldwell, T. E. Cheatham III, W. S. Ross, C. Simmerling, T. Darden, K. M. Merz, R. V. Stanton, A. Cheng, J. J Vincent, M. Crowley D. M. Ferguson, R. Radmer, G. L. Seibel, U. C. Singh, P. Weiner, P. A. Kollman, **1997**, University of California, San Francisco, CA, USA.
[35] W. L. Jorgensen, J. Tirado-Rives, *J. Am. Chem. Soc.* **1988**, *110*, 1657 – 1666.
[36] G. M. Clore, M. Nilges, A. T. Brünger, M. Karplus, A. M. Gronenborn, *FEBS Lett.* **1987**, *213*, 269 – 277.
[37] M. Saunders, K. N. Houk, Y-D. Wu, W. C. Still, M. Lipton, G. Chang, W. C. Guida, *J. Am. Chem. Soc.* **1990**, *112*, 1419 – 1427.
[38] R. Ślusarz, M. J. Ślusarz, R. Kaźmierkiewicz, B. Lammek, *QSAR Comb. Sci.* **2003**, *22*, 865 – 872.

Received on June 6, 2004; Accepted on July 22, 2004

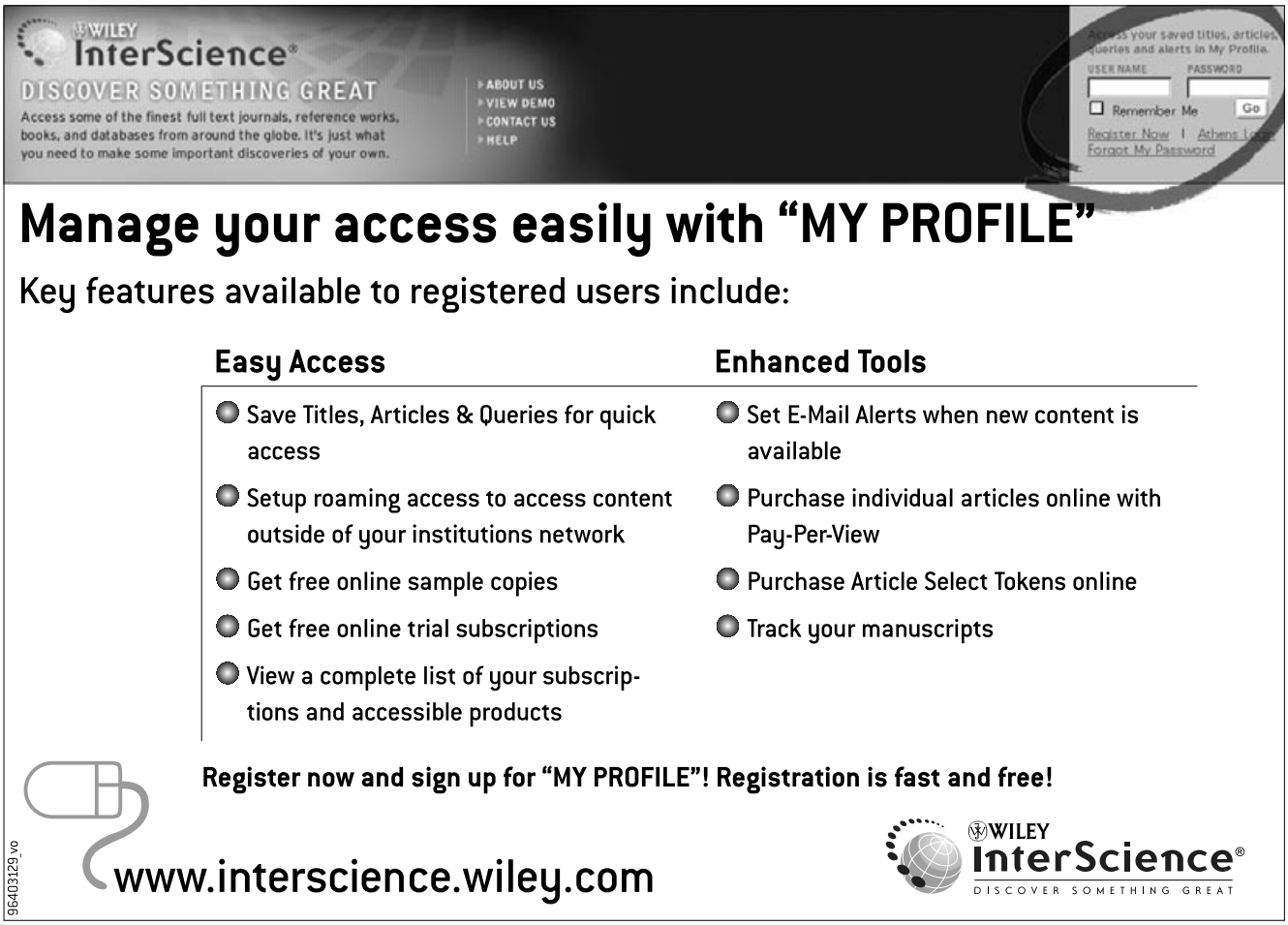


 © 2004 WILEY-VCH Verlag GmbH & Co. KGaA, Weinheim 